GEOS Constituent Data Assimilation Beyond Aura MLS: Assimilating NASA SAGE III/ISS profiles of stratospheric water vapor for continued climate record

K. Emma Knowland[1,2], Pamela A. Wales[1,2], Krzysztof Wargan[2,3], Brad Weir[1,2], Steven Pawson[2], Robert Damadeo[4], David Flittner[4]

[1]Morgan State University, GESTAR-II, Baltimore, Maryland, USA
[2]NASA Goddard Space Flight Center, Global Modeling and Assimilation Office, Greenbelt, Maryland, USA
[3]Science Systems Association, Inc. (SSAI), Lanham, Maryland, USA
[4]NASA Langley Research Center, Hampton, Virginia, USA

Key Points:

- Assimilation of SAGE III/ISS water vapor in NASA GEOS model provides a useful constraint on analyzed stratospheric water vapor
- The analyzed fields can bridge the gap between Aura and future missions measuring stratospheric water vapor
- Polar regions and isolated anomalous events, such as Hunga Tonga eruption, may not be fully captured owing to the ISS orbit.

Corresponding author: K. Emma Knowland, k.e.knowland@nasa.gov

Abstract

Stratospheric water vapor (SWV) is a greenhouse gas that has a significant, yet uncertain, impact on the Earth's climate through its radiative effect and feedback. As the climate changes, it is thus critical to monitor and understand changes in SWV. NASA's Microwave Limb Sounding (MLS) aboard the Aura satellite has observed SWV since 2004 but will soon reach end of life. The Stratospheric Aerosol and Gas Experiment (SAGE) missions observe SWV as well, with the SAGE III instrument operating on the International Space Station (ISS) since 2017. We use the constituent data assimilation capabilities of NASA's Goddard Earth Observing System (GEOS) to demonstrate that the up to 30 SAGE III/ISS profiles each day provide a useful constraint on SWV over the observed midlatitudes and tropics. We conclude that assimilating SAGE III/ISS SWV into GEOS can continue the SWV climate data record of Aura MLS.

Plain Language Summary

Water vapor in the lowest most part of the atmosphere is an integral part of our global weather systems. In the stratosphere, water vapor is low compared to the troposphere (where weather happens) and yet increases can cause increases in tropospheric temperature and reduce stratospheric temperatures. Monitoring stratospheric water vapor is important to our assessment of climate variability and climate change. As NASA's Earth Observing System (EOS) mission satellites come to the end of their missions, our ability to monitor stratospheric water vapor from space will decrease. Here, we show how the infrequent but high quality observations from the Stratospheric Aerosol and Gas Experiment (SAGE) III instrument on the International Space Station until at least 2026 (ISS is expected to be decommissioned in approximately 2030) can be used in a data assimilation system to continue monitoring stratospheric water vapor following the end of the EOS mission satellites.

1 Introduction

Stratospheric water vapor (SWV) is a greenhouse gas that has a significant, yet uncertain, impact on the Earth's climate through its radiative effect and feedback (Gettelman et al., 2010; Solomon et al., 2010; H. J. R. Wang et al., 2020; Xia et al., 2021). SWV is expected to increase (Gettelman et al., 2010) with a positive feedback on surface temperatures. An unexpected decrease in SWV during the early 2000s and its impact on climate is documented (W. J. Randel et al., 2006; Rosenlof & Reid, 2008; Solomon et al., 2010). However, the long-term trend for SWV is contested (Lossow et al., 2019; Yue et al., 2019) depending on the observation source, such as from NOAA's frost-point hygrometers (FPH) (e.g., Hurst et al., 2011) or single- or merged-satellite datasets (e.g., Hegglin et al., 2014; W. Randel & Park, 2019; Konopka et al., 2022). As the climate changes, it is critical to monitor and understand changes in SWV for accurate climate assessments.

The Stratospheric Aerosol and Gas Experiment (SAGE) missions have been instrumental in monitoring the state of stratospheric composition (e.g., Davis et al., 2017; Hegglin et al., 2014; Solomon et al., 2010), yet there was a gap in the SAGE missions from 2005 to 2017. Since the end of 2004, NASA's Aura satellite mission observes SWV using the Microwave Limb Sounder (MLS; Waters et al., 2006) but is nearing its end of life (Fisher, 2017). In order to assess the long-term trends in global SWV, the SAGE and Aura missions must be considered together. It is crucial to establish a long-term record of SWV behaviour while the current SAGE III instrument installed on the International Space Station (ISS) and Aura are both operating in order to reliably assess the newest SAGE record.

Global reanalysis products, such as those produced using NASA's Goddard Earth Observing System (GEOS), are ideal candidates to assess global trends in water vapor.

GEOS uses data assimilation, an application of Bayesian inference (Jazwinski, 1970), to combine and propagate in space and time information from observations using the governing equations from the atmospheric state and estimates of their errors. The GEOS atmospheric data assimilation system (ADAS; Todling & El Akkraoui, 2018), developed and maintained at NASA's Global Modeling and Assimilation Office (GMAO), is able to harmonize multiple sensors to statistically optimize the best representation of global distributions provided as a four-dimensional (4D) product. This method has the potential to generate high spatiotemporal resolution global distributions of atmospheric composition even from relatively sparse data by updating the prior conditions obtained from previous assimilation steps.

Historically, SWV observations have not been included in global reanalyses, resulting in poor representations of SWV fields (Davis et al., 2017). Among those reanalyses, NASA GMAO's Modern-Era Retrospective analysis for Research and Applications, Version 2 (MERRA-2; Gelaro et al., 2017) is one of the better representations of SWV because of its relaxation to a data-driven climatology (Davis et al., 2017). The recently released MERRA-2 Stratospheric Composition REanalysis with Aura MLS (M2-SCREAM; Wargan et al., 2023) is among the first to provide a reanalysis which constrains SWV with space-based measurements (see also BRAM2: Belgian Assimilation System for Chemical ObsErvations Reanalysis of Aura MLS, version2; Errera et al., 2019). M2-SCREAM uses an extension to the GEOS ADAS, the Constituent Data Assimilation system (CoDAS; Wargan et al., 2020; Weir et al., 2021). CoDAS enables the assimilation of satellite retrievals of trace gas abundances within a chemistry mechanism that is coupled to the GEOS atmospheric general circulation model (AGCM).

The assimilation of SAGE water vapor is possible in the CoDAS framework to carry-on the trend and climate assessments after the Aura mission. Previous studies of pre-Aura datasets suggest the atmospheric lifetime of SWV may be long enough that even the limited 15-30 observations a day provided by solar occultation measurements could provide a meaningful constraint on reanalysis fields (Chipperfield et al., 2002; Pierce et al., 2007; Stajner & Wargan, 2004; Stajner et al., 2006). The aim of this study is to test and evaluate if the observations from SAGE will be able to anchor the assimilation system to produce reasonable analyzed water vapor fields.

2 Data

2.1 SAGE III/ISS

The SAGE III instrument was installed on the ISS in February 2017, with measurements available starting in June 2017. The benefit of the SAGE series instruments is the design of the solar occultation technique and the self-calibration of the instruments which supports consistency across the SAGE platforms (H.-J. Wang et al., 2006; Yang et al., 2006). SAGE III/ISS observes between about $\pm$ 70° latitude (H. J. R. Wang et al., 2020) with usually 15 to 30 profiles per day (Davis et al., 2021). The measurements are mainly in the stratosphere, with large uncertainties reported in the troposphere and mesosphere (Damadeo et al., 2018; Davis et al., 2021; McCormick et al., 2020; H. J. R. Wang et al., 2020).

Early validations of SAGE III/ISS water vapor (Davis et al., 2021; Park et al., 2021) demonstrate the success of the mission to continue the high quality, high vertical resolution measurements of stratospheric composition by SAGE occultation instruments. We focus on the SWV profiles using SAGE III/ISS version 5.2 data (hereafter, simply referred to as SAGE) on a 0.5 km grid and we applied the additional filtering recommended by Davis et al. (2021). Our study will cover July 2017 through December 2022.

2.2 Independent observations

2.2.1 Water vapor soundings

Balloon-based frost-point hygrometer instruments measure temperature and water vapor (usually up to the mid-stratosphere) using temperature-moderated mirrors with a thin layer of dew or ice in equilibrium with the air around it. NOAA's FPH (e.g., Vömel et al., 1995; Hall et al., 2016) are routinely launched from Boulder, Colorado, USA (40° N, 105° W); Hilo, Hawaii, USA (20° N, 155° W); and Lauder, New Zealand (45° S, 170° E). Along with the NOAA FPH data, 'cryogenic' frost-point hygrometers (CFH; Vömel et al., 2007) sounding data from Lindenberg, Germany (52.2° N, 14.1° E), San Jose, Costa Rica (10°N, 84.1° W), and Beltsville, Maryland, USA (39.1° N, 76.9° W) are available on routine basis and obtained for the study period.

2.2.2 ACE-FTS

The Atmospheric Chemistry Experiment (ACE) Fourier Transform Spectrometer (FTS) instrument on the Canadian SCISAT satellite measures water vapor using solar occultation. Because of the SCISAT satellite orbit the ACE-FTS measurements observe each latitude during specific times of the year including polar regions, with limited coverage over the tropics (`https://ace.uwaterloo.ca/mission_orbit.php`). The ACE-FTS record begins in 2004, and it is documented to be stable and with a general high bias in SWV but within 10 % when compared against MLS (v3.3/3.4) and other independent observations (P. E. Sheese et al., 2017). We use ACE-FTS version 5.2 data with the quality flags applied (P. Sheese & Walker, 2023).

2.2.3 MLS version 5

MLS provides approximately 3000 profiles per day, with a vertical resolution on the order of 2-3 km, between ± 82° latitude. Version 4.2 water vapor (assimilated in M2-SCREAM) has a documented drift since 2010 when compared against independent observations that results in a wet bias throughout the stratosphere (Hurst et al., 2014, 2016; Livesey et al., 2021; W. Randel & Park, 2019). MLS v5 largely reduces the post-2010 bias to below statistically significant levels when compared to ACE-FTS but still shows significant (though reduced) drifts when compared to FPH stations (Livesey et al., 2021).

2.3 GEOS Reanalysis products

MERRA-2 is a global reanalysis that extends from the surface to the mesosphere and from January 1980 to the present. The MERRA-2 system assimilates a wide range of conventional observations and radiance data to constrain the meteorology (Gelaro et al., 2017). MERRA-2 does not assimilate SWV; instead it applies a 3-day relaxation to a monthly climatology (Davis et al., 2017) and constrains the water mass balance throughout the column (Takacs et al., 2016).

Here, we use the GEOS CoDAS multi-species M2-SCREAM reanalysis water vapor 3D fields (GMAO, 2022; Wargan et al., 2023) as our benchmark of a composition reanalysis appropriate for climate studies. M2-SCREAM is constrained to analyzed meteorological fields from MERRA-2 using the computationally-efficient meteorological "replay" technique (Orbe et al., 2017). M2-SCREAM uses a full stratospheric chemistry mechanism, "StratChem" (Douglass et al., 1997; Kawa et al., 1995; Nielsen et al., 2017; Pawson et al., 2008) and assimilates MLS v4.2 water vapor for the Aura period (2005-one month lag; Wargan et al., 2020, 2023).

3 Methods

In order to be as comparable to M2-SCREAM as possible, the existing GEOS CoDAS infrastructure used to assimilate MLS water vapor in M2-SCREAM was used, following minor adaptation to ingest data from the SAGE instrument. As in the M2-SCREAM system, the experiments assimilated SWV in StratChem with the meteorological replay to MERRA-2 (winds, temperature, pressure, and tropospheric water vapor) at 50 km horizontal resolution.

A series of experiments was conducted:

1. *SAGE assim*: SAGE water vapor GEOS CoDAS assimilation,
2. *MLS assim*: MLS (v5.0) water vapor GEOS CoDAS assimilation, and
3. *Control*: Meteorological replay with StratChem, no assimilation

Each run is initialized from M2-SCREAM fields starting on July 1, 2017. The first half of July 2017 had optimal number of profiles (between 15-30 per day); however, few profiles were collected in the second half of July 2017 (see Figure S1). The SAGE III/ISS instrument has periodic expected interruptions to the observation record, including during summer and winter when the Solar Beta Angle is high ($|\beta| > 60°$; `https://asdc.larc.nasa.gov/documents/sageiii-iss/guide/ReleaseNotes_G3B_v05.30.pdf`). Loss of data constraints, especially for extended periods of time, must be taken into consideration when evaluating the success of any assimilation system (Cohn & Dee, 1988). The SAGE assimilation and the Control were run through December 2022. The MLS v5 assimilation was conducted for a two-year period ending July 2019.

4 Results and Discussion

SWV mixing ratios from M2-SCREAM and the three experiments described in Section 3 are compared against co-located ACE-FTS measurements for 2018 in the range of ± 70° latitude (Figure 1, Table S1). In comparison to the Control experiment (Figure 1a), there is a clear improvement in the distribution of water vapor in the lower stratosphere (blue and cyan dots, 400 and 500 K) in all three assimilation products (Figure 1b-d, see also statistics in Table S1). While the correlation (r) between the assimilated water vapor and ACE-FTS measurements, listed in Figure 1b-d, is greater at higher altitudes (r ranges from 0.88 to 0.94; 1000 and 800 K) compared to the lower stratosphere (r ranges from 0.48 to 0.76; 400 and 500 K), the data constraints drastically improve on the spread compared to the the Control simulation in the lower stratosphere ($r = 0.28$ and 0.39, 400 and 500 K, respectively, Figure 1a).

It is important to remember how the differences among the independent observations can affect the evaluation of the SAGE assimilation. The SAGE analyzed water vapor fall in between the two MLS version estimates relative to ACE-FTS (Figure 1b-d, Table S1), with generally higher estimates in the SAGE assimilation compared to the MLS (v5) assimilation throughout most of the stratosphere (Figure 1b,d; see also Figure S2 zonal mean plots).

To investigate these differences further, FPH and CFH data are used for the period July 2017 through December 2021. The stratospheric profiles shown in Figure 2 are oriented relative to the tropopause altitude. In general, there is good agreement between the station data and the SAGE analyzed water vapor in the stratosphere (6 to 15 km above tropopause; Figure 2a,b). In this altitude range, the mean SAGE analyzed water vapor is within a few tenths of a ppmv of the mean station data, and the standard deviation is generally less than ± 0.5 ppmv (thick black dashed lines), consistent with the results of Davis et al. (2021) which found the SAGE observations were generally within 0.5 ppmv of the balloon-based measurements. In the lowermost stratosphere (0 to 5 km

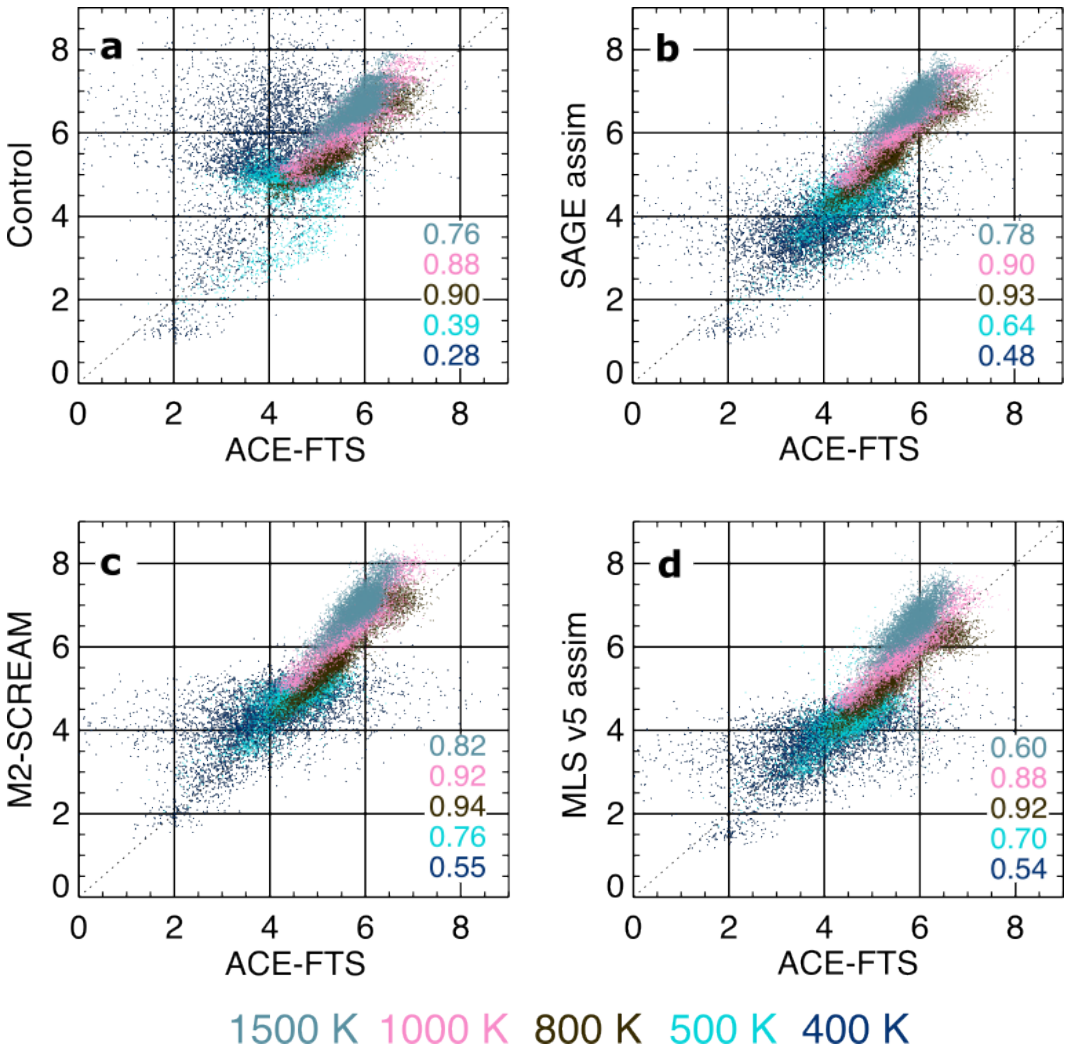

Figure 1. Comparison of 2018 ACE-FTS water vapor to the three experiments and the reanalysis (**a**) Control, (**b**) SAGE assimilation, (**c**) M2-SCREAM, and (**d**) MLS assimilation, sampled at the closest time and location to the ACE-FTS measurements. Five isentropic surfaces in the stratosphere were used: 1500 K (grey), 1000 K (pink), 800 K (black), 500 K (cyan), and 400 K (blue). Inset in each panel provides the Pearson correlation coefficient (r) at each isentropic level. Standard deviation and mean bias at each level are provided in Table S1.

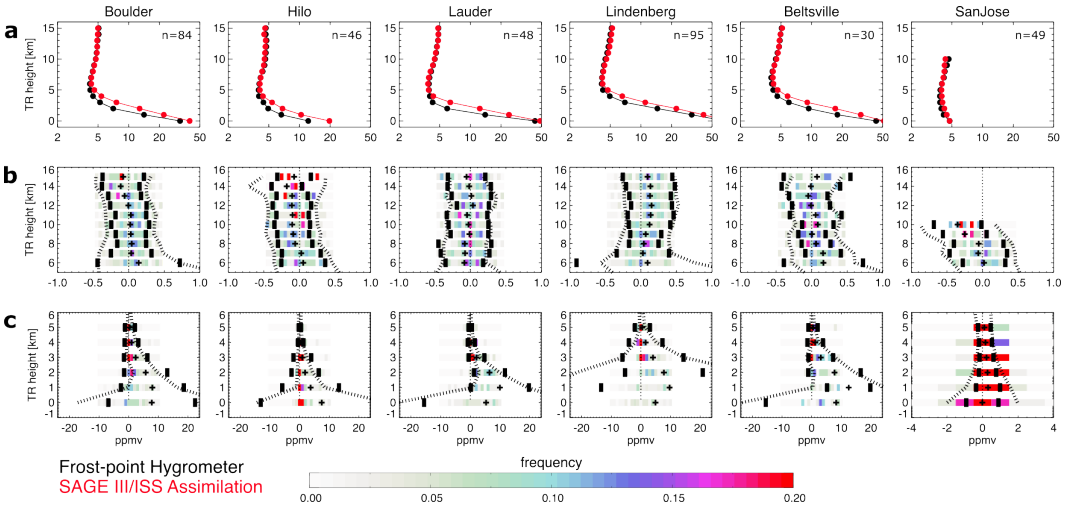

Figure 2. Statistical comparisons of SWV soundings from sites using FPH (Boulder: n=84 profiles, Hilo: 46, Lauder: 48) and CFH (Lindenberg: 95, Beltsville: 30, and San Jose: 49) instruments and SAGE assimilation for July 2017 through December 2021 in troposphere-relative (TR) coordinates. **a**: Mean profiles for station data (black circles) and SAGE assimilation (red circles). **b, c**: Frequency of the differences (model minus observation) are shown for 6 to 15 km (bin size = 0.1 ppmv) and 0 to 5 km (bin size is 0.5 ppmv), respectively. At each km above the tropopause, the mean (crosses), ± 1 standard deviation of the difference (thick black dashed lines), and ± 1 standard deviation of the observations (dotted lines) are indicated. Note, the x-axis in **b** and **c** and for San Jose in **c** are different.

above tropopause; Figure 2a,c), there is a clear transition to higher water vapor estimates in the SAGE assimilation compared to the hygrometer measurements and there is a large increase in the variability of the observations (dotted lines). Except at San Jose, the spread in the differences increases with the standard deviation in the analyzed water vapor fields also increasing, reflecting the observed variability at these levels.

One of the main transport pathways for tropospheric water vapor into the stratosphere is through tropical upwelling as part of the larger Brewer-Dobson circulation (Holton et al., 1995; Mote et al., 1996; W. Randel & Park, 2019). This can be captured through the "tape recorder" signal (Mote et al., 1996), which is the seasonal imprint of tropical tropopause temperatures on SWV, presented here as anomalies in water vapor within ± 15° latitude of the equator (Figure 3). There is relatively dry air leaving the tropopause centered on boreal winter (shown in brown) and relatively moist air in a period centered on boreal summer (blue), which are both advected upward for about an 18 month cycle (Mote et al., 1996; Blunden et al., 2023). In MERRA-2, the tropospheric water vapor is constrained by observations; thus, the annual cycle is well captured between 100 and 70 hPa (Figure 3a). Above about 70 hPa there is little inter-annual variability as mixing ratios are relaxed to a climatology. For M2-SCREAM and the SAGE assimilation, new patterns emerge compared to MERRA-2, indicating that the wet and dry phases can have varying intensities throughout the stratosphere (70 to 10 hPa). While the tape recorder signal in the SAGE assimilation does not appear as smooth as M2-SCREAM, likely due to less frequent tropical observations, the SAGE assimilation is still able to capture it until early 2022.

In January 2022, Hunga Tonga-Hunga Ha'apai (HT-HH), a submarine volcano in the tropical Pacific Ocean (approximately 20° S, 175° W), erupted, injecting vast amounts

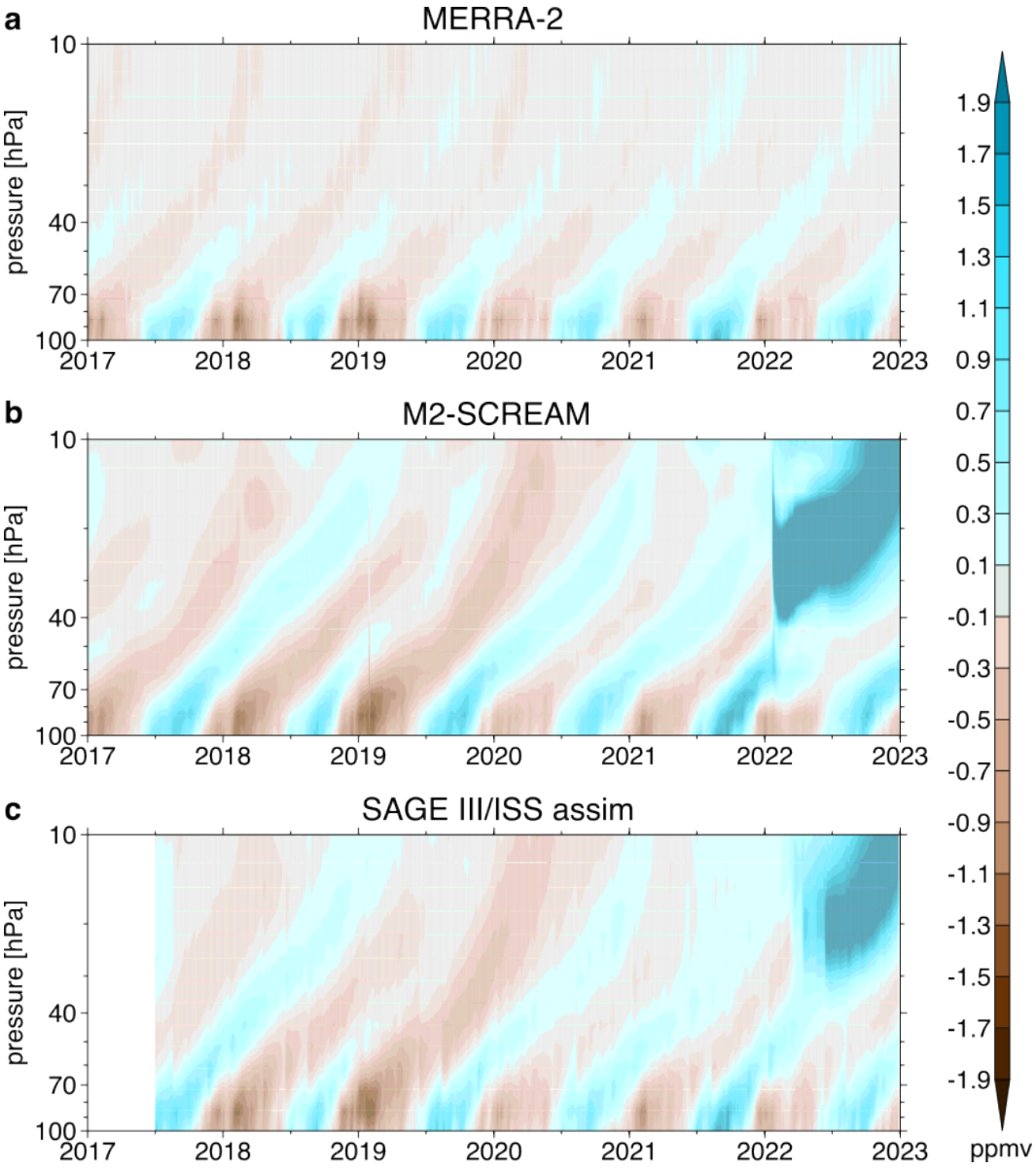

Figure 3. Tropical tape recorder signal assessed as anomalies in water vapor for 15° S to 15° N and 100 to 10 hPa for (**a**) MERRA-2, (**b**) M2-SCREAM, and (**c**) SAGE assimilation for the period of January 1, 2017 through December 31, 2022. The base period for the anomalies do not include 2022: MERRA-2 and M2-SCREAM use the average water vapor for the 5-year period from January 1, 2017 through December 31, 2021, and SAGE assimilation use the average water vapor for the 4-year period from July 2, 2017 through July 1, 2021.

of water into the stratosphere (e.g., Carr et al., 2022; Coy et al., 2022; Manney et al., 2023; Millán et al., 2022; Schoeberl, Wang, Ueyama, Taha, & Yu, 2023; Vömel et al., 2022). In the two assimilation products, the expected vertical transport, as seen in the MERRA-2 reanalysis (Figure 3a) was disrupted above 70 hPa in the early 2022, with anomalously high water vapor now present in the stratosphere (Figure 3b,c). The HT-HH eruption is a natural experiment of how well SAGE captures an anomalous event which can impact Earth's climate (Jenkins et al., 2023; Millán et al., 2022; Schoeberl, Wang, Ueyama, Dessler, et al., 2023; Sellitto et al., 2022). Along with the water vapor, aerosols from the volcanic eruption reached the stratosphere which can impact the ability of space-based instruments like SAGE to observe the full atmosphere (Damadeo et al., 2013; Davis et al., 2021). Microwave radiances, like those retrieved from MLS, are not affected to the same degree by volcanic sulfate aerosols (Millán et al., 2022). It is evident from Figure 3 that the HT-HH water vapor signal is delayed and not as anomalously-high in the SAGE assimilation compared to the assimilation system with MLS (M2-SCREAM, Figure 3b,c). This reduced HT-HH signal led to the following questions:

1. Are there enough SAGE tropical profiles following the HT-HH eruption that the assimilation system would be able to pick up its signal?
2. Does CoDAS need further tuning to handle such extremes?

In Figure 4, the mean zonal analyzed water vapor in the latitude range coinciding with the volcanic plume of high SWV (30° S and the Equator) at 20 hPa (the center of positive tropical tape recorder signal in the SAGE assimilation in Figure 3c) highlights how the assimilation system responds to the frequency of the SAGE observations. In M2-SCREAM (assimilating MLS), there is an increase in the mean water vapor in the days following the eruption, reaching nearly 15 ppmv by the end of January 2022. Prior to the eruption, zonal mean SWV from the SAGE assimilation was within 0.5 ppmv of M2-SCREAM (solid blue line vs red line) and continued at background levels in the immediate months following the eruption, with the few observations available (grey bars) making no impact on the analyzed water vapor (solid blue line, Figure 4). It is not until early March 2022 that SWV in the SAGE assimilation starts to increase each time there are tropical observations (Figure 4). To answer the first question, there are not enough observations of the plume.

In June 2022, the SWV in the austral tropics is at a maximum in the SAGE assimilation (Figure 4). The statistical comparison of the SAGE observations to the assimilation products (Figure 5) highlights the low bias of the SAGE assimilation compared to the observations within the water vapor peak in the layer from 20 to 30 hPa. At each level, the dotted lines are the SAGE retrieval uncertainty which are over 10 ppmv between 30 to 50 hPa (Figure 5a,c). From March to June, the thickness of the layer of high uncertainty decreased (as the uncertainty decreased), and the water vapor in this layer in the SAGE assimilation increased (Figure S3a-d). The monthly statistics comparing the observations versus the GEOS assimilated products illustrates that the CoDAS is performing as expected (Figures 5, S3 and S4), answering the second question, such that where the instrument uncertainty is high for the observations available the CoDAS assigns lower weightings to the observations, contributing to a reduced HT-HH signal in the SAGE assimilation. The profiles of SAGE water vapor observations are compared to the M2-SCREAM analysis (assimilates MLS v4.2) in Figure 5c,d. Since there is very good agreement between M2-SCREAM analyzed water vapor and SAGE observations, the observation uncertainty estimates for SAGE are likely too high.

To explore if the CoDAS algorithm would allow these profiles to have a stronger impact on the system if the uncertainty estimates were reduced, the errors were artificially reduced by a factor of 10 where the aerosol extinction (1020 nm) > $1x10^{-3}$ km^{-1}. While this helps to increase the water vapor in the zonal band of 30° S - Equator (solid vs dashed blue lines, Figure 4), the uncertainty estimates are still large (bottom row, Fig-

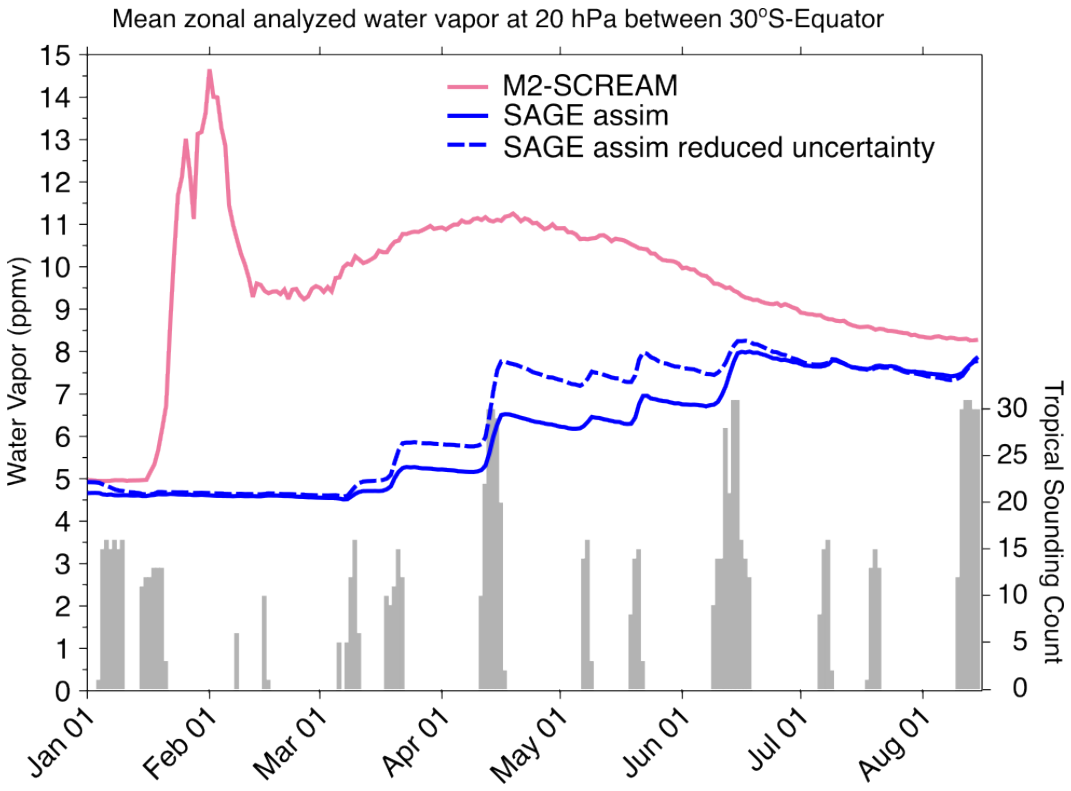

Figure 4. Zonal mean SWV at 20 hPa between 30° S and the Equator for M2-SCREAM (red line), SAGE assimilation (solid blue line) and the SAGE assimilation with the artificially reduced uncertainty (dashed blue line) for January 1 to August 15, 2022. The grey bars indicates the number of daily SAGE profiles in this tropical band.

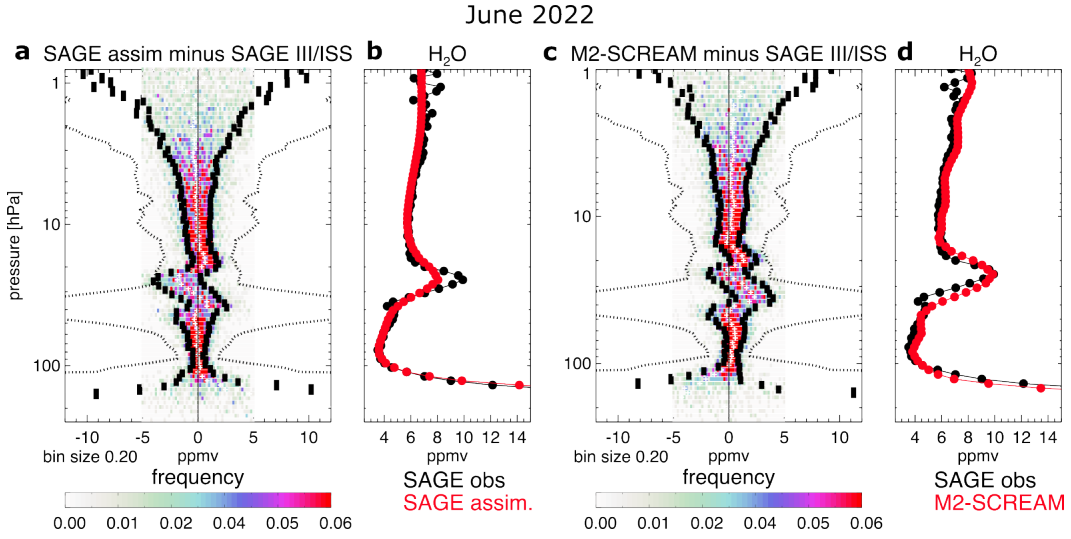

Figure 5. June 2022 tropical SAGE observations compared to analyzed water vapor fields from the SAGE assimilation (**a,b**) and M2-SCREAM (**c,d**). **a,c**: the mean (white crosses), standard deviation (thick black bars), probability density functions (color) of the model minus observation, with SAGE retrieval uncertainty (dotted line). **b,d**: mean SWV profiles.

ure S3) so the assimilation with SAGE water vapor profiles still underestimated the SWV within the plume in comparison to M2-SCREAM (dashed blue vs red lines, Figure 4). By June, as the enhanced aerosol layer sinks (Duchamp et al., 2023) with respect to the water vapor plume, the measurements with high uncertainty are below the enhanced water vapor layer (Figures 5a,b and S3), and the assimilation no longer benefits from the artificially reduced uncertainty (Figure 4). By mid-August, M2-SCREAM and SAGE assimilation estimates are again within 0.5 ppmv.

5 Conclusion

It is critical to monitor and understand changes in stratospheric water vapor (SWV) – a powerful greenhouse gas – as a driver in Earth's evolving climate. For climate assessments, it is critical to have realistic global 3D representation of SWV concentrations. Several Earth-observing satellites have instruments which measure water vapor in the stratosphere; most notably are MLS, ACE-FTS and SAGE series instruments. Both MLS and ACE-FTS are heritage instruments launched in the early 2000s, and at least MLS is nearing the end of its life. Reanalysis products are useful for analyzing long-term variability, but those without observational constraints for SWV are not suitable for scientific studies of SWV (Davis et al., 2017). Two recent reanalyses have included MLS water vapor in the DA observing system (Errera et al., 2019; Wargan et al., 2023). While the community awaits follow-on missions, the assimilation of SAGE SWV profiles should be considered in reanalysis products. This study demonstrated there is a clear benefit to assimilating the SAGE water vapor observations, albeit less frequent with respect to MLS, with the caveat that for anomalous events, like HH-TH eruption, and where there are few to no observations (e.g., seasonally in the tropics, and the polar regions), the reanalysis product would be mainly driven by background fields.

Open Research Section

The Atmospheric Chemistry Experiment (ACE), also known as SCISAT, is a Canadian-led mission mainly supported by the Canadian Space Agency. ACE-FTS Level 2 data was obtained from https://databace.scisat.ca/level2/ and quality flags (P. Sheese & Walker, 2023) were accessed through `https://doi.org/10.5683/SP3/NAYNFE`. SAGE III/ISS is a NASA Langley managed mission funded by the NASA Science Mission Directorate within the Earth Systematic Mission Program. Enabling partners are the NASA Human Exploration and Operations Mission Directorate, the International Space Station Program, and the European Space Agency. SAGE III/ISS is available at `https://doi.org/10.5067/ISS/SAGEIII/SOLAR_NetCDF4_L2-V5.2`. MLS v5 are available from `https://disc.gsfc.nasa.gov/datasets?page=1&source=Aura\%20MLS&project=Aura`. M2-SCREAM is available through the Goddard Earth Sciences Data and Information Services Center (https://disc.gsfc.nasa.gov) and the specific M2-SCREAM product collection used here is cited appropriately in the references as GMAO (2022). FPH observations were obtained from `https://gml.noaa.gov/ozwv/wvap/` using the Water Vapor Data Archive FTP. The CFH observations were obtained from NDACC and can be accessed via this link: `https://ndacc.larc.nasa.gov/instruments/sonde`.

Acknowledgments

Support from the National Aeronautics and Space Association through the SAGE III/ISS Science Team Grant with Program Manager Richard Eckman (80NSSC21K1197,80NSSC23K0510) to GMAO Scientists (K.E.K., P.A.W., K.W., B.W., and S.P.) is gratefully acknowledged. Resources supporting this work were provided by the NASA High-End Computing (HEC) Program through the NASA Center for Climate Simulation at Goddard Space Flight Center (GSFC). The authors thank Holger Vömel for his guidance with the CFH data, and the CFH Beltsville team.

P.A.W. downloaded and prepared the SAGE III/ISS profiles for CoDAS. Updates to CoDAS were made by B.W. Experiments designed and analyzed by GMAO Scientists and carried out by K.E.K., with initial tuning performed by K.W.. Figures by K.E.K. and K.W.. Initial draft written by K.E.K. with contributions from all co-authors.

References

Blunden, J., Boyer, T., & Bartow-Gillies, E. (2023). State of the Climate in 2022. *Bulletin of the American Meteorological Society*, *104*(9), S1 – S516. (Place: Boston MA, USA Publisher: American Meteorological Society) doi: https://doi.org/10.1175/2023BAMSStateoftheClimate.1

Carr, J. L., Horváth, , Wu, D. L., & Friberg, M. D. (2022). Stereo plume height and motion retrievals for the record-setting hunga tonga-hunga ha'apai eruption of 15 january 2022. *Geophysical Research Letters*, *49*(9), e2022GL098131. doi: https://doi.org/10.1029/2022GL098131

Chipperfield, M. P., Khattatov, B. V., & Lary, D. J. (2002). Sequential assimilation of stratospheric chemical observations in a three-dimensional model. *Journal of Geophysical Research*, *107*(D21), ACH 8-1-ACH 8-14. doi: https://doi.org/10.1029/2002JD002110

Cohn, S. E., & Dee, D. P. (1988). Observability of Discretized Partial Differential Equations. *SIAM Journal on Numerical Analysis*, *25*(3), 586–617. doi: https://doi.org/10.1137/0725037

Coy, L., Newman, P. A., Wargan, K., Partyka, G., Strahan, S. E., & Pawson, S. (2022). Stratospheric Circulation Changes Associated With the Hunga Tonga-Hunga Ha'apai Eruption. *Geophysical Research Letters*, *49*(22), e2022GL100982. doi: https://doi.org/10.1029/2022GL100982

Damadeo, R. P., Zawodny, J. M., Remsberg, E. E., & Walker, K. A. (2018). The impact of nonuniform sampling on stratospheric ozone trends derived from occultation instruments. *Atmospheric Chemistry and Physics*, *18*(2), 535–554. doi: https://doi.org/10.5194/acp-18-535-2018

Damadeo, R. P., Zawodny, J. M., Thomason, L. W., & Iyer, N. (2013). SAGE version 7.0 algorithm: application to SAGE II. *Atmospheric Measurement Techniques*, *6*(12), 3539–3561. doi: https://doi.org/10.5194/amt-6-3539-2013

Davis, S. M., Damadeo, R., Flittner, D., Rosenlof, K. H., Park, M., Randel, W. J., ... Vömel, H. (2021). Validation of SAGE III/ISS Solar Water Vapor Data With Correlative Satellite and Balloon-Borne Measurements. *Journal of Geophysical Research*, *126*(2), e2020JD033803. doi: https://doi.org/10.1029/2020JD033803

Davis, S. M., Hegglin, M. I., Fujiwara, M., Dragani, R., Harada, Y., Kobayashi, C., ... Wright, J. S. (2017). Assessment of upper tropospheric and stratospheric water vapor and ozone in reanalyses as part of S-RIP. *Atmospheric Chemistry and Physics*, *17*(20), 12743–12778. doi: https://doi.org/10.5194/acp-17-12743-2017

Douglass, A. R., Rood, R. B., Kawa, S. R., & Allen, D. J. (1997). A three-dimensional simulation of the evolution of the middle latitude winter ozone in the middle stratosphere. *Journal of Geophysical Research: Atmospheres*, *102*(D15), 19217-19232. doi: https://doi.org/10.1029/97JD01043

Duchamp, C., Wrana, F., Legras, B., Sellitto, P., Belhadji, R., & von Savigny, C. (2023). Observation of the Aerosol Plume From the 2022 Hunga Tonga—Hunga Ha'apai Eruption With SAGE III/ISS. *Geophysical Research Letters*, *50*(18), e2023GL105076. doi: https://doi.org/10.1029/2023GL105076

Errera, Q., Chabrillat, S., Christophe, Y., Debosscher, J., Hubert, D., Lahoz, W., ... Walker, K. (2019). Technical note: Reanalysis of Aura MLS chemical observations. *Atmospheric Chemistry and Physics*, *19*(21), 13647–13679. doi: https://doi.org/10.5194/acp-19-13647-2019

Fisher, D. (2017). *Mission Status for Earth Science Constellation MOWG Meeting at KSC: EOS Aura.* Available at: https://ntrs.nasa.gov/citations/20170011627 (last retrieved: October 29, 2020).

Gelaro, R., McCarty, W., Suárez, M. J., Todling, R., Molod, A., Takacs, L., ... Zhao, B. (2017). The Modern-Era Retrospective Analysis for Research and Applications, Version 2 (MERRA-2). *J. Climate*, *30*(14), 5419-5454. doi: https://doi.org/10.1175/JCLI-D-16-0758.1

Gettelman, A., Hegglin, M. I., Son, S.-W., Kim, J., Fujiwara, M., Birner, T., ... Tian, W. (2010). Multimodel assessment of the upper troposphere and lower stratosphere: Tropics and global trends. *Journal of Geophysical Research: Atmospheres*, *115*(D3). doi: https://doi.org/10.1029/2009JD013638

GMAO. (2022). *M2-SCREAM: 3d,3-Hourly,Instantaneous,Model-Level,Assimilation,Assimilated Constituent Fields,Replayed MERRA-2 Meteorological Fields, Greenbelt, MD, USA, [Dataset], Goddard Earth Sciences Data and Information Services Center (GES DISC), Accessed: September 2023.* doi: https://doi.org/10.5067/7PR3XRD6Q3NQ

Hall, E. G., Jordan, A. F., Hurst, D. F., Oltmans, S. J., Vömel, H., Kühnreich, B., & Ebert, V. (2016). Advancements, measurement uncertainties, and recent comparisons of the NOAA frost point hygrometer. *Atmospheric Measurement Techniques*, *9*(9), 4295–4310. doi: https://doi.org/10.5194/amt-9-4295-2016

Hegglin, M., Plummer, D., Shepherd, T., Scinocca, J., Anderson, J., Froidevaux, L., ... others (2014). Vertical structure of stratospheric water vapour trends derived from merged satellite data. *Nature Geoscience*, *7*(10), 768–776.

Holton, J. R., Haynes, P. H., McIntyre, M. E., Douglass, A. R., Rood, R. B., & Pfister, L. (1995). Stratosphere-troposphere exchange. *Reviews of Geophysics*, *33*(4), 403–439. doi: 10.1029/95RG02097

Hurst, D. F., Lambert, A., Read, W. G., Davis, S. M., Rosenlof, K. H., Hall, E. G., ... Oltmans, S. J. (2014). Validation of aura microwave limb sounder stratospheric water vapor measurements by the noaa frost point hygrometer. *Journal of Geophysical Research: Atmospheres*, *119*(3), 1612-1625. doi: https://doi.org/10.1002/2013JD020757

Hurst, D. F., Oltmans, S. J., Vömel, H., Rosenlof, K. H., Davis, S. M., Ray, E. A., ... Jordan, A. F. (2011). Stratospheric water vapor trends over boulder, colorado: Analysis of the 30 year boulder record. *Journal of Geophysical Research*, *116*(D2). doi: https://doi.org/10.1029/2010JD015065

Hurst, D. F., Read, W. G., Vömel, H., Selkirk, H. B., Rosenlof, K. H., Davis, S. M., ... Oltmans, S. J. (2016). Recent divergences in stratospheric water vapor measurements by frost point hygrometers and the aura microwave limb sounder. *Atmospheric Measurement Techniques*, *9*(9), 4447–4457. doi: https://doi.org/10.5194/amt-9-4447-2016

Jazwinski, A. H. (1970). *Stochastic processes and filtering theory.* Academic Press, Inc., New York, NY.

Jenkins, S., Smith, C., Allen, M., & Grainger, R. (2023). Tonga eruption increases chance of temporary surface temperature anomaly above 1.5°C. *Nature Climate Change*, *13*(2), 127–129. doi: https://doi.org/10.1038/s41558-022-01568-2

Kawa, S. R., Kumer, J. B., Douglass, A. R., Roche, A. E., Smith, S. E., Taylor, F. W., & Allen, D. J. (1995). Missing chemistry of reactive nitrogen in the upper stratospheric polar winter. *Geophysical Research Letters*, *22*(19), 2629-2632. doi: https://doi.org/10.1029/95GL02336

Konopka, P., Tao, M., Ploeger, F., Hurst, D. F., Santee, M. L., Wright, J. S., & Riese, M. (2022). Stratospheric Moistening After 2000. *Geophysical Research Letters*, *49*(8), e2021GL097609. (e2021GL097609 2021GL097609) doi: https://doi.org/10.1029/2021GL097609

Livesey, N. J., Read, W. G., Froidevaux, L., Lambert, A., Santee, M. L., Schwartz,

M. J., ... Nedoluha, G. E. (2021). Investigation and amelioration of long-term instrumental drifts in water vapor and nitrous oxide measurements from the Aura Microwave Limb Sounder (MLS) and their implications for studies of variability and trends. *Atmospheric Chemistry and Physics*, *21*(20), 15409–15430. doi: https://doi.org/10.5194/acp-21-15409-2021

Lossow, S., Khosrawi, F., Kiefer, M., Walker, K. A., Bertaux, J.-L., Blanot, L., ... Rosenlof, K. H. (2019). The sparc water vapour assessment ii: profile-to-profile comparisons of stratospheric and lower mesospheric water vapour data sets obtained from satellites. *Atmospheric Measurement Techniques*, *12*(5), 2693–2732. doi: 10.5194/amt-12-2693-2019

Manney, G. L., Santee, M. L., Lambert, A., Millán, L. F., Minschwaner, K., Werner, F., ... Wang, T. (2023). Siege in the Southern Stratosphere: Hunga Tonga-Hunga Ha'apai Water Vapor Excluded From the 2022 Antarctic Polar Vortex. *Geophysical Research Letters*, *50*(14), e2023GL103855. doi: https://doi.org/10.1029/2023GL103855

McCormick, M. P., Lei, L., Hill, M. T., Anderson, J., Querel, R., & Steinbrecht, W. (2020). Early results and validation of SAGE III-ISS ozone profile measurements from onboard the International Space Station. *Atmospheric Measurement Techniques*, *13*(3), 1287–1297. doi: https://doi.org/10.5194/amt-13-1287-2020

Millán, L., Santee, M. L., Lambert, A., Livesey, N. J., Werner, F., Schwartz, M. J., ... Froidevaux, L. (2022). The hunga tonga-hunga ha'apai hydration of the stratosphere. *Geophysical Research Letters*, *49*(13), e2022GL099381. doi: https://doi.org/10.1029/2022GL099381

Mote, P. W., Rosenlof, K. H., McIntyre, M. E., Carr, E. S., Gille, J. C., Holton, J. R., ... Waters, J. W. (1996). An atmospheric tape recorder: The imprint of tropical tropopause temperatures on stratospheric water vapor. *Journal of Geophysical Research*, *101*(D2), 3989-4006. doi: https://doi.org/10.1029/95JD03422

Nielsen, J. E., Pawson, S., Molod, A., Auer, B., da Silva, A. M., Douglass, A. R., ... Wargan, K. (2017). Chemical Mechanisms and Their Applications in the Goddard Earth Observing System (GEOS) Earth System Model. *Journal of Advances in Modeling Earth Systems*, *9*(8), 3019-3044. doi: https://doi.org/10.1002/2017MS001011

Orbe, C., Oman, L. D., Strahan, S. E., Waugh, D. W., Pawson, S., Takacs, L. L., & Molod, A. M. (2017). Large-Scale Atmospheric Transport in GEOS Replay Simulations. *J. Adv. Model. Earth Syst.*. doi: https://doi.org/10.1002/2017MS001053

Park, M., Randel, W. J., Damadeo, R. P., Flittner, D. E., Davis, S. M., Rosenlof, K. H., ... Read, W. (2021). Near-global variability of stratospheric water vapor observed by sage iii/iss. *Journal of Geophysical Research*, *126*(7), e2020JD034274. doi: https://doi.org/10.1029/2020JD034274

Pawson, S., Stolarski, R. S., Douglass, A. R., Newman, P. A., Nielsen, J. E., Frith, S. M., & Gupta, M. L. (2008). Goddard earth observing system chemistry-climate model simulations of stratospheric ozone-temperature coupling between 1950 and 2005. *Journal of Geophysical Research*, *113*(D12). doi: https://doi.org/10.1029/2007JD009511

Pierce, R. B., Schaack, T., Al-Saadi, J. A., Fairlie, T. D., Kittaka, C., Lingenfelser, G., ... Fishman, J. (2007). Chemical data assimilation estimates of continental U.S. ozone and nitrogen budgets during the Intercontinental Chemical Transport Experiment–North America. *Journal of Geophysical Research*, *112*(D12). (D12S21) doi: 10.1029/2006JD007722

Randel, W., & Park, M. (2019). Diagnosing Observed Stratospheric Water Vapor Relationships to the Cold Point Tropical Tropopause. *Journal of Geophysical Research*, *124*(13), 7018-7033. doi: 10.1029/2019JD030648

Randel, W. J., Wu, F., Vömel, H., Nedoluha, G. E., & Forster, P. (2006). Decreases in stratospheric water vapor after 2001: Links to changes in the tropical tropopause and the Brewer-Dobson circulation. *Journal of Geophysical Research*, *111*(D12). doi: https://doi.org/10.1029/2005JD006744

Rosenlof, K. H., & Reid, G. C. (2008). Trends in the temperature and water vapor content of the tropical lower stratosphere: Sea surface connection. *Journal of Geophysical Research*, *113*(D6). doi: https://doi.org/10.1029/2007JD009109

Schoeberl, M. R., Wang, Y., Ueyama, R., Dessler, A., Taha, G., & Yu, W. (2023). The Estimated Climate Impact of the Hunga Tonga-Hunga Ha'apai Eruption Plume. *Geophysical Research Letters*, *50*(18), e2023GL104634. doi: https://doi.org/10.1029/2023GL104634

Schoeberl, M. R., Wang, Y., Ueyama, R., Taha, G., & Yu, W. (2023). The Cross Equatorial Transport of the Hunga Tonga-Hunga Ha'apai Eruption Plume. *Geophysical Research Letters*, *50*(4), e2022GL102443. doi: https://doi.org/10.1029/2022GL102443

Sellitto, P., Podglajen, A., Belhadji, R., Boichu, M., Carboni, E., Cuesta, J., ... Legras, B. (2022). The unexpected radiative impact of the Hunga Tonga eruption of 15th January 2022. *Communications Earth & Environment*, *3*(1), 288. doi: https://doi.org/10.1038/s43247-022-00618-z

Sheese, P., & Walker, K. (2023). *Data Quality Flags for ACE-FTS Level 2 Version 5.2 Data Set.* Borealis. doi: https://doi.org/10.5683/SP3/NAYNFE

Sheese, P. E., Walker, K. A., Boone, C. D., Bernath, P. F., Froidevaux, L., Funke, B., ... von Clarmann, T. (2017). ACE-FTS ozone, water vapour, nitrous oxide, nitric acid, and carbon monoxide profile comparisons with MIPAS and MLS. *Journal of Quantitative Spectroscopy and Radiative Transfer*, *186*, 63-80. (Satellite Remote Sensing and Spectroscopy: Joint ACE-Odin Meeting, October 2015) doi: https://doi.org/10.1016/j.jqsrt.2016.06.026

Solomon, S., Rosenlof, K. H., Portmann, R. W., Daniel, J. S., Davis, S. M., Sanford, T. J., & Plattner, G.-K. (2010). Contributions of Stratospheric Water Vapor to Decadal Changes in the Rate of Global Warming. *Science*, *327*(5970), 1219–1223. doi: https://doi.org/10.1126/science.1182488

Stajner, I., & Wargan, K. (2004). Antarctic stratospheric ozone from the assimilation of occultation data. *Geophysical Research Letters*, *31*(18). (L18108) doi: https://doi.org/10.1029/2004GL020846

Stajner, I., Wargan, K., Chang, L.-P., Hayashi, H., Pawson, S., & Nakajima, H. (2006). Assimilation of ozone profiles from the improved limb atmospheric spectrometer-ii: Study of antarctic ozone. *Journal of Geophysical Research*, *111*(D11). (D11S14) doi: https://doi.org/10.1029/2005JD006448

Takacs, L. L., Suárez, M. J., & Todling, R. (2016). Maintaining atmospheric mass and water balance in reanalyses. *Quarterly Journal of the Royal Meteorological Society*, *142*(697), 1565-1573. doi: https://doi.org/10.1002/qj.2763

Todling, R., & El Akkraoui, A. (2018). *The GMAO hybrid ensemble-variational atmospheric data assimilation system: Version 2.0. In NASA technical report series on global modeling and data assimilation, NASA/TM-2018-104606.* https://gmao.gsfc.nasa.gov/pubs/docs/Todling1019.pdf.

Vömel, H., David, D. E., & Smith, K. (2007). Accuracy of tropospheric and stratospheric water vapor measurements by the cryogenic frost point hygrometer: Instrumental details and observations. *Journal of Geophysical Research*, *112*(D8). doi: https://doi.org/10.1029/2006JD007224

Vömel, H., Evan, S., & Tully, M. (2022). Water vapor injection into the stratosphere by Hunga Tonga-Hunga Ha'apai. *Science*, *377*(6613), 1444-1447. doi: https://doi.org/10.1126/science.abq2299

Vömel, H., Oltmans, S. J., Hofmann, D. J., Deshler, T., & Rosen, J. M. (1995). The evolution of the dehydration in the Antarctic stratospheric vortex. *Journal of Geophysical Research*, *100*(D7), 13919-13926. doi: https://doi.org/10.1029/

95JD01000

Wang, H.-J., Cunnold, D. M., Trepte, C., Thomason, L. W., & Zawodny, J. M. (2006). SAGE III solar ozone measurements: Initial results. *Geophysical Research Letters*, *33*(3). (L03805) doi: https://doi.org/10.1029/2005GL025099

Wang, H. J. R., Damadeo, R., Flittner, D., Kramarova, N., Taha, G., Davis, S., ... Hall, E. (2020). Validation of SAGE III/ISS Solar Occultation Ozone Products With Correlative Satellite and Ground-Based Measurements. *Journal of Geophysical Research*, *125*(11), e2020JD032430. (e2020JD032430 2020JD032430) doi: https://doi.org/10.1029/2020JD032430

Wargan, K., Weir, B., Manney, G. L., Cohn, S. E., Knowland, K. E., Wales, P. A., & Livesey, N. J. (2023). M2-SCREAM: A Stratospheric Composition Reanalysis of Aura MLS Data With MERRA-2 Transport. *Earth and Space Science*, *10*(2), e2022EA002632. doi: https://doi.org/10.1029/2022EA002632

Wargan, K., Weir, B., Manney, G. L., Cohn, S. E., & Livesey, N. J. (2020). The Anomalous 2019 Antarctic Ozone Hole in the GEOS Constituent Data Assimilation System With MLS Observations. *Journal of Geophysical Research: Atmospheres*, *125*(18), e2020JD033335. doi: https://doi.org/10.1029/2020JD033335

Waters, J. W., Froidevaux, L., Harwood, R. S., Jarnot, R. F., Pickett, H. M., Read, W. G., ... Walch, M. J. (2006, May). The Earth Observing System Microwave Limb Sounder (EOS MLS) on the Aura Satellite. *IEEE Transactions on Geoscience and Remote Sensing*, *44*(5), 1075–1092.

Weir, B., Crisp, D., O'Dell, C. W., Basu, S., Chatterjee, A., Kolassa, J., ... Ott, L. E. (2021). Regional impacts of COVID-19 on carbon dioxide detected worldwide from space. *Science Advances*, *7*(45), eabf9415. doi: https://doi.org/10.1126/sciadv.abf9415

Xia, Y., Wang, Y., Huang, Y., Hu, Y., Bian, J., Zhao, C., & Sun, C. (2021). Significant Contribution of Stratospheric Water Vapor to the Poleward Expansion of the Hadley Circulation in Autumn Under Greenhouse Warming. *Geophysical Research Letters*, *48*(17), e2021GL094008. Retrieved from `https://agupubs.onlinelibrary.wiley.com/doi/abs/10.1029/2021GL094008` (e2021GL094008 2021GL094008) doi: https://doi.org/10.1029/2021GL094008

Yang, E.-S., Cunnold, D. M., Salawitch, R. J., McCormick, M. P., Russell, J., Zawodny, J. M., ... Newchurch, M. J. (2006). Attribution of recovery in lower-stratospheric ozone. *Journal of Geophysical Research*, *111*(D17). (D17309) doi: https://doi.org/10.1029/2005JD006371

Yue, J., Russell III, J., Gan, Q., Wang, T., Rong, P., Garcia, R., & Mlynczak, M. (2019). Increasing Water Vapor in the Stratosphere and Mesosphere After 2002. *Geophysical Research Letters*, *46*(22), 13452-13460. doi: https://doi.org/10.1029/2019GL084973